

Solar Cells for Sustainable Development: Applications and the Materials Used for Fabrication

Sani Garba Danjumma

Department of Sciences,
Kebbi State Polytechnic, Dakingari, Nigeria.

Saidu Aliyu

Department of Sciences,
Kebbi State Polytechnic, Dakingari, Nigeria.

Mamuda Buhari

SRBS,
Federal Polytechnic, Kaura Namoda, Nigeria.

Sahabi Suleiman

Department of Sciences,
Kebbi State Polytechnic, Dakingari, Nigeria.

Abubakar Ibrahim

Department of Sciences,
Kebbi State Polytechnic, Dakingari, Nigeria

Abstract—With the ever increasing demand for energy, the search for alternative energy sources has increased. The worldwide use of fossil fuels has led to the critical situation of global warming, significantly affecting our health, environment and climate. Extensive emphasis have been put on the implementation of renewable energy sources and solar energy is by far the most abundant form of renewable energy. Solar cells convert sunlight directly to electricity and can be influential in meeting the world's energy demand. Solar cells provide power for lighting, communications, electricity for remote areas, disaster relief, scientific experiments, water Pumping, charging vehicle batteries, signal systems, refrigerators, small DC appliances, ATMs and telephone booths etc. So many materials are found useful in solar cells fabrications among which are silicon oxides, cadmium sulphide, copper sulphide, cuprous sulphide, nickel oxide, zinc oxide, silver nanoparticles, titanium dioxides, lead, gallium arsenide, perovskite, graphene, gold cores, aluminium oxide, copper oxide, zinc sulphide, cadmium telluride and copper indium diselenide. For cumulative capacity for PV, the top countries were China, the United States, Japan, Germany and Italy, with India not far behind. It is therefore recommended that, government should invest in this sector considering the huge applications and abundant materials used in fabrication for sustainable development.

Keywords—Solar cells, sustainable development, applications, materials, fabrication

I. INTRODUCTION

In recent years, photovoltaic cell technology has grown extraordinarily as a sustainable source of energy, as a consequence of the increasing concern over the impact of fossil fuel-based energy on global warming and climate change. Our nations limits mercury, lead, sulfur, and other dangerous air pollutants and is now poised to deal with the carbon emissions hastening climate change. The best way to do that is a strong embrace of energy efficiency to make our homes and buildings more comfortable using less energy, as well as advance clean energy sources such as solar. Solar energy is by far the most abundant form of renewable energy and has the potential to partially replace fossil fuels. The amount of solar radiation striking our earth's surface is about ten thousand times higher than the current global electrical energy consumption and solar cells is one of the way to harness solar energy.

The materials most commonly used are silicon (si) and compounds of cadmium sulphide (CdS), cuprous sulphide (Cu₂S) and gallium arsenide (GaAs) (Shruti *et al.*, 2015). Earlier photovoltaic solar cells are thin silicon wafers that transform sunlight energy into electrical power. The modern photovoltaic technology is based on the principle of electron hole creation in each cell composed of two different layers (p-type and n-type materials) of a semiconductor material. When a photon of sufficient energy impinges on the p-type and n-type junction, an electron is ejected by gaining energy from the striking photon and moves from one layer to another. This creates an electron and a hole in the process and by this process electrical power is generated (Choubey *et al.*, 2012). The various types of materials applied for photovoltaic solar cells includes mainly in the form of silicon (single crystal, multi-crystalline, amorphous silicon), cadmium-telluride, copper-indium-gallium-selenide, and copper-indium-gallium-sulfide. On the basis of these materials, the photovoltaic solar cells are categorized into various classes as shown in Fig. 1.1.

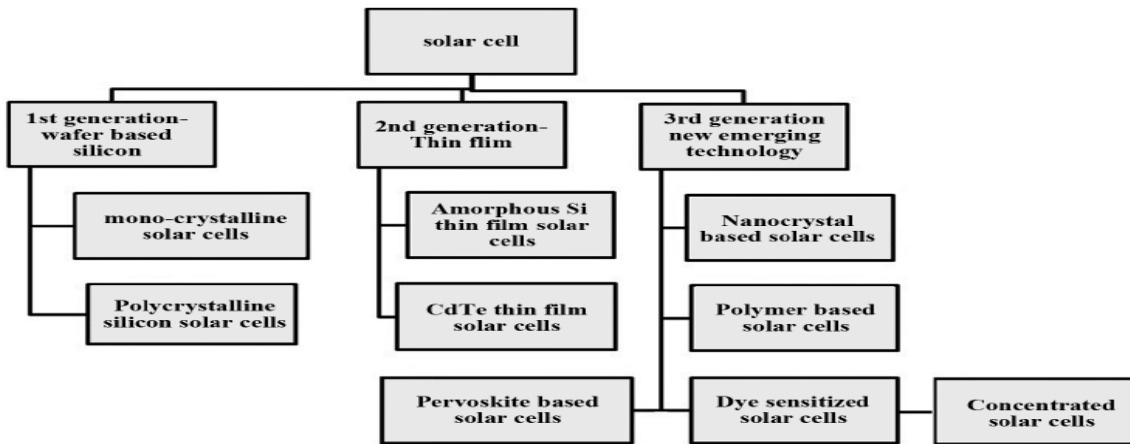


Fig. 1.1: Various types of solar cell technologies and current trends of development (Shruti *et al.*, 2015).

The first generation solar cells are produced on silicon wafers. It is the oldest and the most popular technology due to high power efficiencies. The silicon wafer based technology is further categorized into two subgroups named as Mono-crystalline silicon solar cell and Multi-crystalline silicon solar cell. Mono crystalline solar cell, as the name indicates, is manufactured from single crystals of silicon by a process called Czochralski process. Polycrystalline PV modules are generally composed of a number of different crystals, coupled to one another in a single cell. The processing of polycrystalline Si solar cells is more economical, which are produced by cooling a graphite mold filled containing molten silicon. Polycrystalline Si solar cells are currently the most popular solar cells (Shruti *et al.*, 2015).

Most of the thin film solar cells and a-Si are second generation solar cells, and are more economical as compared to the first generation silicon wafer solar cells. Silicon-wafer cells have light absorbing layers up to 350 μm thick, while thin-film solar cells have a very thin light absorbing layers, generally of the order of 1 μm thickness. Thin film solar cells are classified as Amorphous Silicon Thin Film (a-Si) Solar Cell, Cadmium Telluride (CdTe) and Copper Indium Gallium Di-Selenide (CIGS) Solar Cells. The third generation cells are the new promising technologies which are yet to be commercially investigated in detail and they include Nano crystal based solar cells, Polymer based solar cells, dye sensitized solar cells and concentrated solar cells (Shruti *et al.*, 2015). A number cadmium telluride and copper indium di-selenide are now being used for PV modules. The attraction of these technologies is that they can be manufactured by relatively inexpensive, yet they typically offer higher module efficiency than amorphous silicon (Soteris, 2009).

Nura and Kamarulazizi (2015), evaluated the transmission efficiency and optical concentration ratio of the Bee-eyes array of Fresnel lenses for solar photovoltaic concentrator system with the number of zones ranging from 1 to 20. Bee-eyes array Fresnel lenses concentrator provide high concentration factor which is greater than 1000x at the 20th zone. In addition, the system also provides room for increasing the number of zones to achieve the high

concentration factor if needs arise. The transmission efficiency greater than 90% has been achieved with f - number of ≥ 1.25 and the transmission efficiency greater than 75% can be maintained with acceptance angle larger than 1.5° where this shows that hexagonal Fresnel lenses are suitable for moderate concentrated photovoltaic systems.

José *et al.* (2019), classified photovoltaic cells developed up to date into four main categories called generations (GEN), and clarified that, the current market is mainly covered by the first two GEN. The 1GEN (mono or polycrystalline silicon cells and gallium arsenide) comprises well-known medium/low cost technologies that lead to moderate yields. The 2GEN (thin-film technologies) includes devices that have lower efficiency albeit are cheaper to manufacture. The 3GEN presents the use of novel materials, as well as a great variability of designs, and comprises expensive but very efficient cells. The 4GEN, also known as “inorganics-in-organics”, combines the low cost/flexibility of polymer thin films with the stability of novel inorganic nanostructures (i.e., metal nanoparticles and metal oxides) with organic-based nanomaterials (i.e., carbon nanotubes, graphene and its derivatives), and are currently under investigation. They concluded that, in the next future and after comprehensive research on the field, 4GEN PSCs incorporating carbon-based nanomaterials would offer high performance levels to rival those of traditional silicon-based cells, thus providing a new outlook for the solar energy industry.

A. An Excerpt of the Renewables 2018: Global Status Report on Solar PV Capacity (REN21, 2018)

The year 2017 was a landmark one for solar photovoltaics (PV): the world added more capacity from solar PV than from any other type of power generating technology. More solar PV was installed than the net capacity additions of fossil fuels and nuclear power combined. In 2017, solar PV was the top source of new power capacity in several major markets, including China, India, Japan and the United States. Globally, at least 98 GWdc of solar PV capacity was installed (on- and off-grid), increasing total capacity by nearly one-third, for a cumulative total of approximately 402 GW as shown in Fig. 1.2.

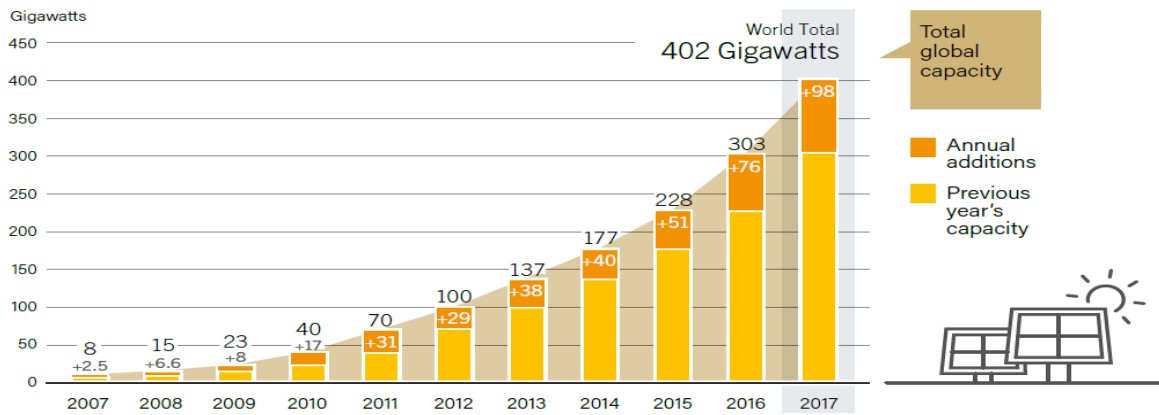


Fig. 1.2: Solar PV Global Capacity and Annual Additions, 2007-2017

On average, the equivalent of more than 40,000 solar panels was installed each hour of the year. The significant market increase relative to 2016 was due primarily to China, where new installations were up more than 50%. India's market doubled, while other major markets (Japan and the United States) contracted. For the fifth year running, Asia eclipsed all other regions, accounting for 75% of global additions. The top five national markets – China, the United States, India, Japan and Turkey – were responsible for nearly 84% of newly installed capacity; the next five were Germany, Australia, the Republic of Korea,

the United Kingdom and Brazil. For cumulative capacity, the top countries were China, the United States, Japan, Germany and Italy, with India not far behind (see Fig. 1.3). Despite the heavy concentration in a handful of countries, new markets are emerging and countries on all continents have begun to contribute significantly to global growth. By the end of 2017, every continent had installed at least 1 GW and at least 29 countries had 1 GW or more of capacity. The leaders for solar PV capacity per inhabitant were Germany, Japan, Belgium, Italy and Australia

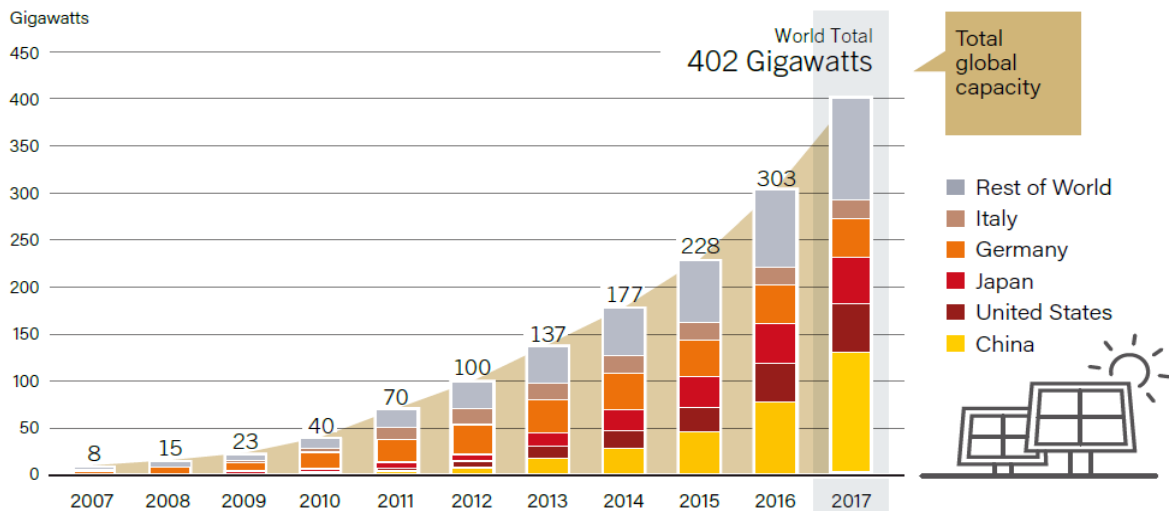


Fig. 1.3: Solar PV Global Capacity, by Country or Region, 2007-2017

II. APPLICATIONS OF SOLAR CELLS

PV systems are being used in a variety of applications

A. Lighting

With the invention of LED (light emitting diode) technology as low power lighting sources, PV systems find an ideal application in remote or mobile lighting systems. PV systems combined with battery storage facilities are mostly used to provide lighting for billboards, highway information signs, public-use facilities, parking lots, lighting for trains (Satheesh, 2018; Lewis and Larry, 2010).

B. Communications

Signals required by communication systems need amplification after particular distance intervals. Various relay towers are stationed to boost radio, television, and phone signals. High grounds are mostly favoured as the sites for repeater stations. These sites are generally far from power lines. To reduce the difficulty and cost associated with generators, PV systems are being installed as a viable alternative (Satheesh, 2018). Because of the high cost of inputs and the manufacturing process, GaAs cell adoption has been limited to communication and military satellite applications. (Silicon Valley Toxics Coalition, 2009).

C. Electricity for remote areas

Some areas are quite far from the distribution network to establish connection with the grid. Areas under construction also need power supply before they are connected. PV systems are an attractive option for these cases. Furthermore, PV systems can be backed up by conventional generators to provide uninterrupted supply (Satheesh, 2018; Soteris, 2009 and Lewis and Larry, 2010).

D. Disaster Relief

Natural calamities often bring about an electricity crisis. As the disasters such as hurricanes, floods, tornadoes, and earthquakes destroy electricity generation and distribution systems. In situations like these, where power will be out for an extended period, portable PV systems can provide temporary solutions for light, communication, food and water systems. Emergency health clinics opt for PV based electricity over conventional systems in lieu of problems of fuel transport and pollution (Satheesh, 2018; Lewis and Larry, 2010).

E. Scientific experiments

In various cases, scientific experiments are set up in areas far from power supply. PV systems can be effectively used to carry out scientific activities in remote areas. Systems monitoring seismic activities, highway conditions, meteorological information and other research activities can be powered by PV systems (Satheesh, 2018; Soteris, 2009).

F. Signal Systems

Navigational systems, such as light houses, highway and aircraft warning signals can be far from the electric grid. PV systems can be a reliable power source for these important applications. Even portable traffic lights can be powered by PV systems (Satheesh, 2018; Soteris, 2009).

G. Water Pumping

PV is a perfect candidate for agricultural and livestock purposes due to the need for water during the periods with bright sunshine. These pumping systems can supply water directly to fields, or can store water for the time of need. These systems can even be used to provide water to remote areas and villages (Satheesh, 2018).

H. Charging Vehicle Batteries

Vehicles running on electric power can be charged at PV powered stations. Such vehicles can also maintain their critical battery states using PV powered sources. Boats and other leisure vehicles can be charged directly using PV systems (Satheesh, 2018; Soteris, 2009).

I. Consumer Products and Public utilities

PV technology is being used for variety of commercially available consumer based products. Small DC appliances such as toys, watches, calculators, radios, televisions, flashlights, fans etc. can operate with PV based energy systems. Various public utility systems such as teller machines and telephone booths can also be powered by PV

systems (Satheesh, 2018; Abdin, *et al.*, 2013). Amorphous silicon (a-Si) solar PV cells are widely used to power small, low-power consumer devices like watches, calculators, and outdoor lighting (Silicon Valley Toxics Coalition, 2009). Lead is often used in solar PV electronic circuits for wiring, solder-coated copper strips, and some lead-based printing pastes. (Silicon Valley Toxics Coalition, 2009).

III. MATERIALS USED FOR FABRICATION

So many materials are reported to be useful in solar cells fabrication. Among which are reviewed in this paper and are classified as follows:

A. Silicon based solar cells

As it is already mentioned, the first generation solar cells are produced on silicon wafers. It is the oldest and the most popular technology due to high power efficiencies. The silicon wafer based technology is further categorized into two subgroups named as Mono-crystalline silicon solar cell and Multi-crystalline silicon solar cell (Shruti *et al.*, 2015). The black silicon exhibits an excellent optical performance but its overall power conversion efficiency is quite low. The increased surface area due to nanostructures increases surface recombination and the better diffusion of dopants due to increased surface area and structured defects cause high doping regions which leads to Auger recombination. Poor metal contacts also cause electrical losses. Although the electrical performance is quite poor but due to high optical performance there are future possibilities to improve the electrical properties of Black silicon along with maintaining its optical properties to make black silicon as a future material for solar cells (Mayank and Reeta, 2017).

Amorphous silicon (a-si) is a glassy alloy of silicon and hydrogen (about 10%). Several properties make it an attractive material for thin film solar cells. Silicon is abundant and environmentally friendly. Amorphous silicon absorbs sun light extremely well, so that only a very thin active solar cell layer is required, thus greatly reducing solar cell material requirements. Amorphous silicon (a-Si) solar PV cells are widely used to power small, low-power consumer devices like watches, calculators, and outdoor lighting. This non-crystalline form of silicon is applied as a thin film to various surfaces. Amorphous silicon cells have been commercially available since the 1970s, and they are relatively inefficient at converting sunlight to electricity (reaching a maximum of about 12 percent). However, because they are a thousand times thinner than c-Si cells, they use less silicon and are much cheaper to produce. They can also be made more efficient by stacking with other thin-film semiconductors. Gallium arsenide (GaAs) is currently used in multi-junction solar PV cells, combined with thin-film materials such as cadmium telluride (CdTe), amorphous silicon (a-Si), aluminum indium phosphide (AlInP), aluminum gallium indium phosphide (AlGaInP), or gallium indium phosphide (GaInP) (Silicon Valley Toxics Coalition, 2009).

Fig. 3.1 shows Global market share of solar PV semiconductors. Crystalline silicon (c-si) occupies the largest with 89.6% followed by amorphous silicon (a-si) with 5.2%. cadmium tellurite (CdTe) occupies 4.7%, copper indium selenide (CIS)/copper indium gallium selenide occupies 0.5% and others (allium arsenide, zinc manganese tellurium, indium gallium phosphide/germanium, and indium gallium nitride) occupies less than 0.1%. This shows that c-si is the most utilised worldwide for solar PV semiconductors (Silicon Valley Toxics Coalition, 2009).

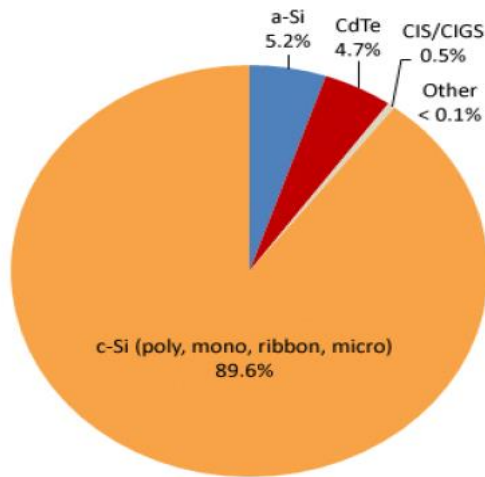


Figure 3.1: Global Market Share of Solar PV Semiconductors in 2007 (Silicon Valley Toxics Coalition, 2009).

Low pressure chemical vapour deposition (LP-CVD) ZnO as front transparent conductive oxide (TCO), developed at IMT, has excellent light-trapping properties for a-Si:H p-i-n single-junction and ‘micromorph’ (amorphous/microcrystalline silicon) tandem solar cells. A stabilized record efficiency of 9.47% has independently been confirmed by NREL for an amorphous silicon single junction p-i-n cell (1 cm²) deposited on LP-CVD ZnO coated glass. Micromorph tandem cells with an initial

efficiency of 12.3% show after light-soaking a stable performance of 10.8% (Meier *et al.*, 2004). Fig. 3.2 shows for the tandem cell a high initial efficiency of over 12% combined with a high open circuit voltages of 1.4 V. After the light soaking stability test an efficiency of 10.8% could be measured.

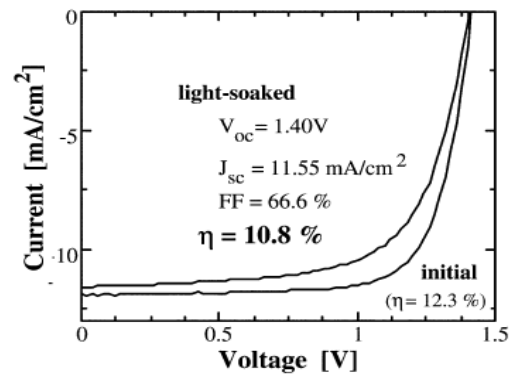


Fig. 3.2: AM1.5 I-V characteristics of a micromorph tandem test cell deposited on glassyLP-CVD ZnO in the initial state and after 1000 h of light-exposure (1 sun at 50 8C). The mc-Si:H bottom cell has a thickness of 2 nm (Meier *et al.*, 2004).

Adriano and Izete (2012), developed silicon solar cell processes based on low cost chemicals and gases as well as gettering mechanisms and fabricated more than 12,000 solar cells, achieving efficiencies up to 16%, and two hundred photovoltaic modules were produced and characterized. The yield of solar cell fabrication was of 86% and standard deviation of the module nominal power was of around 2.5%, which denotes the high reproducibility of the developed processes. Fig. 3.3 show the comparison I-V characteristics of npn cells and npp cells. Cell 2 and cell 4 were measured at CalLab - FhG-ISE and cell 1 and cell 3 were the best efficiency (η) achieved of 16.1% and 13.4% for cells with and without back surface field, respectively. Fill factors of around 0.78 were obtained as a result of the optimized screen-printing metal grid.

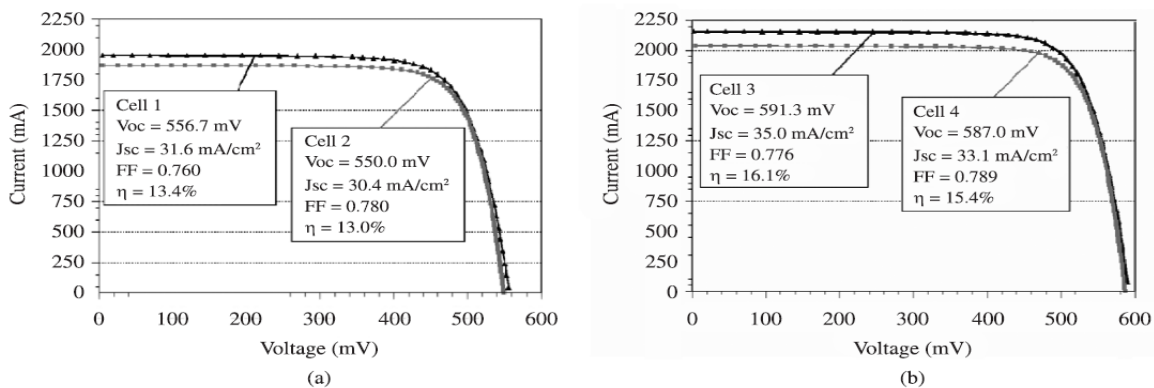


Fig. 3.3: Electrical characteristics at standard conditions of a) n+pn+ and b) n+pp+ solar cells (Adriano and Izete, 2012).

Holly *et al.* (2016), demonstrate improved light trapping in dye-sensitized solar cells (DSSCs) with hybrid bimetallic gold core/silver shell nanostructures. Silica-coated bimetallic nanostructures (Au/Ag/SiO₂ NSs) integrated in the active layer of DSSCs resulted in 7.51% power

conversion efficiency relative to 5.97% for reference DSSCs, giving rise to 26% enhancement in device performance. Photocurrent spectra of the best performing DSSCs (Fig. 3.4) demonstrate that maximum plasmonic enhancement is achieved for DSSCs containing 0.44 wt wt Au/Ag/SiO₂ nanostructures reaching a maximum PCE of

7.51%, which is 26% higher than the 5.97% PCE achieved with the reference DSSC.

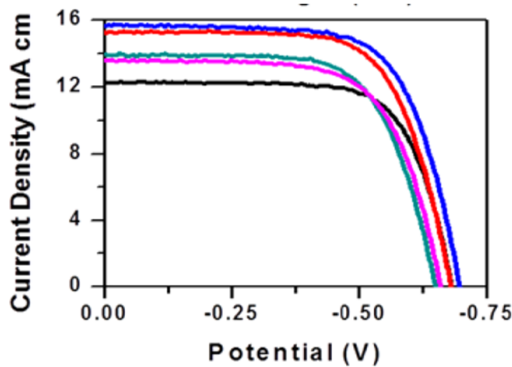


Fig. 3.4: Corresponding current density spectra of the devices (Holly *et al.*, 2016).

Plakhotnyuk *et al.* (2016), present recent results of lifetime optimization for nano-structured black silicon and its photovoltaic applications. They clarified that, black silicon nano-structures provide significant reduction of silicon surface reflection due to highly corrugated nanostructures with excellent light trapping properties. Lifetime measurements resulted in 1220 μs and to 4170 μs for p- and n-type CZ silicon wafers, respectively. They concluded that, this is promising for use of black silicon RIE nano-structuring in a solar cell process flow.

Fig. 3.5 shows measured effective minority carrier lifetime for p- and n-type wafers for polished as well as for nano-textured samples Plakhotnyuk *et al.* (2016).

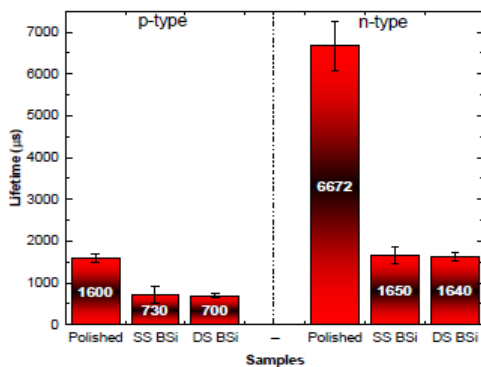


Fig. 3.5: Comparative graph of average lifetime wafer mapping values with standard deviation for p- and n-type silicon samples with polished, single side nanostructured and double side nanostructured black silicon, passivated with ALD Al_2O_3 37 nm film. Legend: SS BSi - single side nanostructured black silicon, DS BSi-double side nano-structured black silicon (Plakhotnyuk *et al.*, 2016).

B. Gallium Arsenide Based Solar Cells

Anil *et al.* (2001), emphasize that, measurement of solar cell ac parameters is important for the design of efficient and reliable satellite power systems. In their study, the ac parameters of Gallium Arsenide (GaAs/Ge) solar cell have been measured using impedance spectroscopy. The cell capacitance, dynamic resistance, and series resistance were measured. The results show that the transition capacitance (C_T) is dominant up to 0.9 V and beyond 0.9 V diffusion capacitance is significant. The experimental values of cell resistance are in good agreement with calculated cell resistance, as shown in Fig. 3.6.

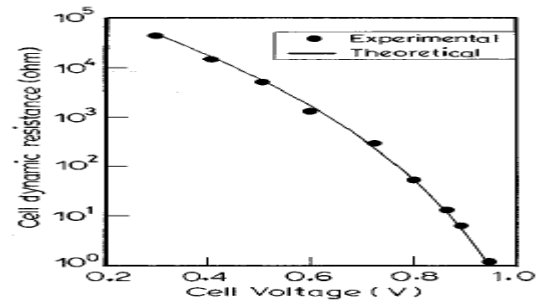


Fig. 3.6. Comparison of cell resistance (experimental and theoretical) at different cell voltage (V_d) (Anil *et al.*, 2001).

Davood *et al.* (2011), described a novel PV solar cell structure consisting of an HJ of a-Si:H on GaAs. Solar cells using this structure were successfully fabricated at $<200^\circ\text{C}$. It was shown that epitaxial Si can be grown on GaAs at $<200^\circ\text{C}$ under PECVD conditions with high dilution ratio. Two structures were proposed and studied employing both epi-Si and a-Si:H on GaAs. The electrical data from HJ GaAs structures with epi-Si are shown to offer better performance to that with conventional HJ GaAs structure with a-Si:H due to reduced optical losses and parasitic series resistance in the former. It is clear from the data that further improvement in conversion efficiency requires much more effective surface passivation of the HJ interface.

The 1 sun $J-V$ characteristics from the samples with different hydrogen dilution ratios are shown in Fig. 3.7. It is evident from the light $J-V$ data that sample 2 with the highest hydrogen dilution level of 10 has the highest short circuit current density J_{sc} , while sample 1 with the lowest hydrogen dilution level of 2 has the highest open circuit voltage (V_{oc}).

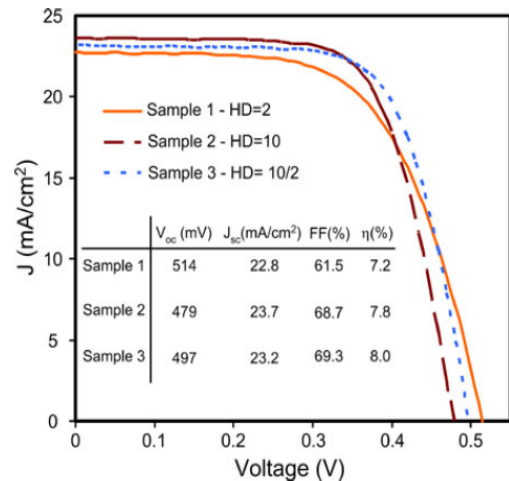


Fig. 3.7: Light $J-V$ characteristics of the different HJ GaAs cells measured at 1 sun (Davood *et al.* 2011).

Jonathan *et al.* (2012), demonstrated light absorption enhancement on a 100 nm, a 500 nm, and a 1000 nm thick GaAs solar cell structure featuring a back reflector, a double-layer anti reflection coating, and a close-packed silica nanosphere array. It was observed that, the thinner the cell, the more the potential for improvement. They observed the highest improvement of 11% for the 100-nm GaAs solar cell by adding 700-nm hexagonally close-

packed SiO₂ nanospheres on top of it. They also see that depending on the size of the spheres, the enhancement they obtain occurs on different parts of the spectrum. Therefore, the best current densities are obtained where WGMs enhance the weakly absorbing region of the active material.

Vishnuvardhanan and Dunbar (2013), investigated the technical feasibility of the tandem solar cell. They reported on the detailed electrical and optical simulations of this structure quantifying various theoretical and practical loss mechanisms in the interface and in the device and indicate that an efficiency improvement of 5.13% would be attainable with present generation of gallium arsenide and silicon solar cells in this configuration.

The GaAs solar cells are grown by low-pressure metal organic chemical vapour deposition (LP-MOCVD) and fabricated by photolithography, metal evaporation, annealing, and wet chemical etch processes. Anodized aluminium oxide (AAO) masks are prepared from an aluminium foil by a two-step anodization method. Photovoltaic and optical characteristics of the GaAs solar cells with and without the nanohole arrays are investigated where the short-circuit current density seem to increased up to 11.63% and the conversion efficiency improved from 10.53 to 11.57% under 1-sun AM 1.5G conditions by using the nanohole arrays. These results show that the nanohole arrays fabricated with an AAO technique may be employed to improve the conversion efficiency of the GaAs solar cell. The total conversion efficiency of the solar cell with the deeper nanohole arrays shows a higher value compared to that of the planar or shallow patterned solar cell, as shown in Figure 3.8 (Kangho *et al.*, 2013).

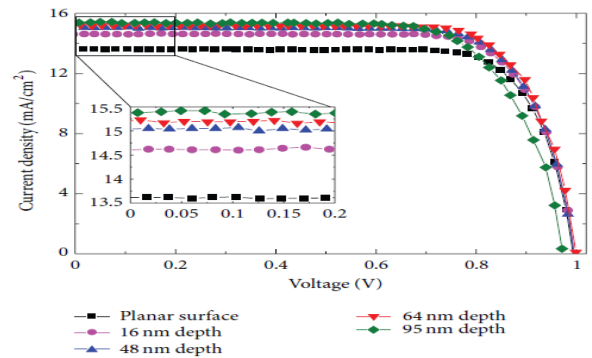


Figure 3.8: J-V curves of the GaAs solar cells with and without the nanohole arrays (Kangho *et al.*, 2013).

Mrityunjoy *et al.* (2015), presented improvement performance of GaAs solar cell of antireflection coating and texturing using PC1D simulation. About 32.58% light reflect from a bare GaAs surface and giving external quantum efficiency about 67.32%. They presented the improvement of external quantum efficiency (EQE) of GaAs solar cell about 14.23% using antifriction coating (ARC) of Silicon-di-Oxide (SiO₂) with refractive index of 1.55 at thickness 121 nm and about 14.77% using ARC of and Indium Tin Oxide (ITO) with refractive index 1.92 at 100 nm.

Mahfoud *et al.* (2015), simulated the top GaInP and the bottom GaAs tandem cells separately using the one dimensional solar simulator SCAPS-1D. The temperature dependency of the solar cell's characteristics was investigated in the temperature range from 25 to 80°C. The simulation results show that voltage losses within the tandem cell are additive (Top cell and Bottom cell), while the short circuit current density depends smoothly on temperature, and the efficiency reduction is about (-0.038), (-0.035) and (-0.054 % / °C) for the bottom, top and tandem cells respectively. The matching current becomes dependent on the top cell, since this last has smaller variation compared with the bottom cell. Fig. 3.9. Show a slight increase of the short-current density in both Top and Bottom cells.

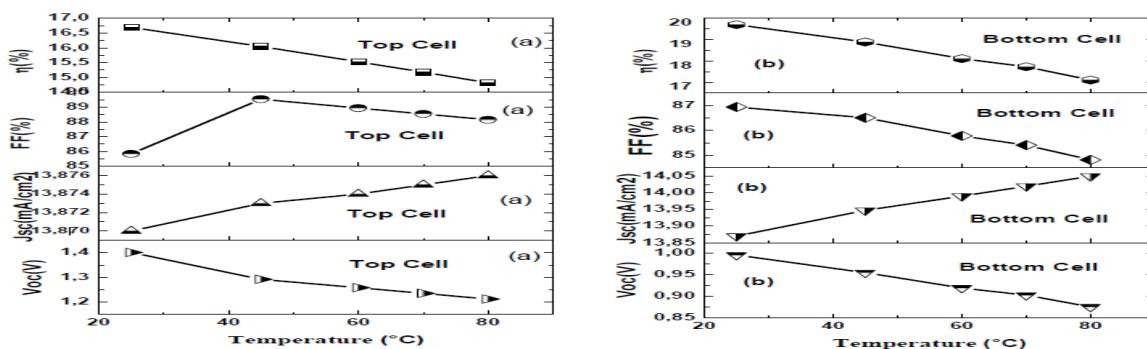


Fig. 3.9. Temperature dependence of the characteristics Voc, Jsc, FF and η for solar cell: (a) Top cell, (b) Bottom cell (Mahfoud *et al.*, 2015).

Xiaoqiang, *et al.* (2018), clarified that, the honeycomb connection of carbon atoms by covalent bonds in a macroscopic two-dimensional scale leads to fascinating grapheme and solar cells based on graphene/silicon Schottky diode have been widely studied. For solar cell applications, GaAs is superior to silicon as it has a direct band gap of 1.42 eV and its electron mobility is six times

that of silicon. However, graphene/GaAs solar cell has been rarely explored. They reported that, graphene/GaAs solar cells have conversion efficiency (η) of 10.4% and 15.5% without and with anti-reflection layer on graphene, respectively. The η of 15.5% is higher than the state of art efficiency for graphene/Si system (14.5%). Furthermore, their calculation points out η of 259.8% can be reached by reasonably optimizing the open circuit

voltage, junction ideality factor, resistance of graphene and metal/graphene contact. They concluded that, graphene/GaAs heterostructure solar cell have great potential for practical applications.

The application of AR-coating on the front surface of the GaAs solar cell, gives very encouraging results. The current density is increased from 15.37 mA/cm^2 to 27.48 mA/cm^2 at 75 nm thicknesses for ARC Si_3N_4 film and to 29.55 mA/cm^2 after adding surface texturing. The efficiency is increased from 14.89% to 27.16% for Si_3N_4 ARC and to 29.57% after making texturing to the front ARC surface (Mostafa *et al.*, 2018).

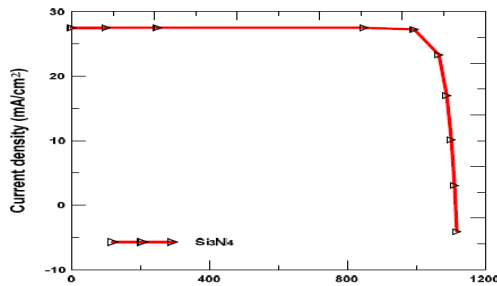


Fig. 3.10. JV characteristics for GaAs solar cell with Si_3N_4 ARC layer

Fig. 3.10, the J-V characteristic of the proposed solar cell is presented. The simulation results show that the maximum efficiency than can be achieved is 27.16% , the open circuit voltage is 1.1 V and the short circuit current density is 27.52 mA/cm^2 (Mostafa *et al.*, 2018).

C. Cadmium Based Solar Cells

$\text{Cu}_2\text{S}/\text{CdS}$ heterojunction has been prepared and characterized by using the vacuum evaporation technique on glass substrate. The Cu_2S layer was obtained by the dry method, i.e. by evaporation of a CuCl film followed by heat treatment. The photovoltaic properties including I-V characteristics, short-circuit current (I_{sc}), open-circuit voltage (V_{oc}), fill factor (ff), efficiency (η) of $\text{Cu}_2\text{S}/\text{CdS}$ heterojunction cells have been examined after formation. It was observed that, heat treatment improved the photovoltaic cells. High resistivity of CdS thin film, high series resistance and the poor design of the grid have led to low efficiency (Ashour, 2006).

Ezenwa and Okereke (2011), deposited Cadmium sulphide (CdS), copper sulphide (CuS) and (CdS/CuS) thin films on glass substrate using the chemical bath deposition. Optical and morphological characterisation of the films were carried out using a Janway 6405 UV/VIS spectrometer and an olumpus optical microscope. Optical transmittance in the spectral region from 400 nm to 680 nm was studied. Optical constant such as extinction coefficient and refractive index were evaluated. The optical band gap energy were found to be 2.40 eV for CdS , 2.30 eV for CuS and 2.45 eV for CdS/CuS thin films. They therefore concluded that, the results clearly shows the feasibility of using these materials for photovoltaic applications.

Cadmium telluride (CdTe) thin films are prepared by the dip-coating deposition technique under atmospheric pressure at different temperature. The optical band gap obtained within the range $1.63\text{-}1.60 \text{ eV}$. The cadmium telluride (CdTe) thin films are found to be good

photoconductive in nature and could be used in photovoltaic applications. The current-voltage (I-V) characteristic of the device consisting of $\text{ITO}/\text{CdTe}/\text{Au}$ of two films prepared at two different backing temperatures are shown in Fig. 3.11. The photocurrent is measured using a light source having power of 100 watt white bulb for the films deposited at 250°C baking temperature as shown in Fig. 3.11 (Sekhar and Kaushik, 2013).

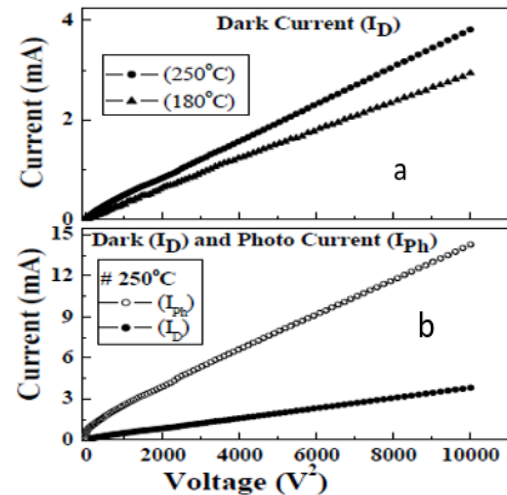


Fig. 3.11: (a) Voltage-Current ($V\text{-}I$) relationship (dark current) of CdTe films (b) Dark (I_D) and photocurrent (I_{Ph}) of the CdTe film (Sekhar and Kaushik, 2013).

The most dramatic advancements in CdTe device efficiencies were made during the 2013 to 2014 time frame when small-area cell conversion efficiency was raised to 20% range and a champion module efficiency of 17% was reported. CdTe technology is attractive in terms of its limited life-cycle greenhouse gas and heavy metal emissions, small carbon footprint, and short energy payback times (Bülent and Brian, 2014).

Enam *et al.* (2017), investigated the conventional CdTe based solar cells with modified silicon tandem structure using the numerical analysis. In their AMPS-1D simulation, the thickness of $n\text{-Si}$, $p\text{-Si}$ and $p\text{-CdTe}$ layer have been varied and the optimum cell output parameters have been found. The simulated results have shown that the tandem structure enhances the efficiency. The final solar cell output parameters such as $V_{oc} = 1.15 \text{ V}$, $J_{sc} = 27.612 \text{ mA/cm}^2$ & $FF = 0.894$ with an increased conversion efficiency of 28.457% are obtained as compared with the basic CdTe solar cell efficiency of 19.701% . Moreover, the conversion efficiency linearly decreases with the increase of operating temperature with a temperature coefficient of $-0.15\%/^\circ\text{C}$, which also indicates the better degree of stability of the cell at higher operating temperature or in stressed conditions. Therefore, it is hoped that with the modified CdTe structure, an efficient and cost effective CdTe/Si tandem thin film solar cell can be realized using basic fabrication methods for practical usage in near future. The light J-V curve and External Quantum Efficiency (EQE) graph of the baseline CdTe and modified CdTe structure with silicon wafer found by AMPS-1D simulation are shown in Fig. 3.12.

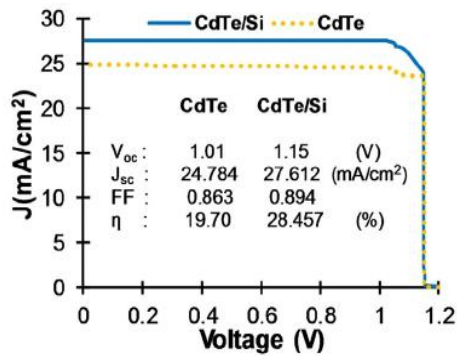


Fig. 3.12. J-V characteristics of both CdTe & CdTe/Si tandem solar cell structure Enam *et al.* (2017).

Karla *et al.* (2018), observed that the inclusion of an undoped SnO₂ buffer layer to form SnO₂/CdS led to an appreciable increase of the open circuit voltage and a moderate increase in the Jsc. The increase in series resistance caused by the introduction of the additional layer is more than compensated by the Voc and Jsc increases. Overall, the efficiency of the cell improved from 2.1% to 3.7%. These changes promoted by the buffer layer are probably due to passivation effects of the SnO₂/CdS interface, blocking of diffusion impurities from the substrate or to improvement of the band alignment. Dark and illuminated I-V curves of the two heterostructures (with and without u-SnO₂ layer) are displayed in Fig. 3.13.

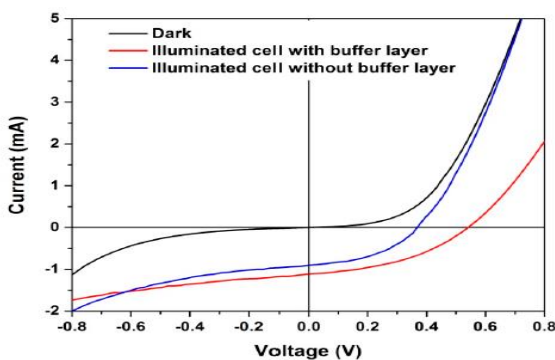


Figure 3.13: Dark and illuminated I-V curves of the heterostructures (Karla *et al.*, 2018).

D. Perovskite and Titanium Dioxide Based Solar Cells

Perovskites are a class of compounds defined by the formula ABX₃ where X represents a halogen such as I⁻, Br⁻, Cl⁻ and A and B are cations of different size. Perovskite solar cells are recent discovery among the solar cell research community and possess several advantages over conventional silicon and thin film based solar cells (Shruti *et al.*, 2015).

Gold nanoparticles were incorporated into TiO₂ nanoparticles for dye-sensitized solar cells (DSSCs). At the optimum Au/TiO₂ mass ratio of 0.05, the power-conversion efficiency of the DSSC improved to 3.3% from a value of 2.7% without Au, and this improvement was mainly attributed to the photocurrent density. The Au

nanoparticles embedded in the nanoparticulate-TiO₂ film strongly absorbed light due to the localized surface-plasmon resonance, and thereby promoted light absorption of the dye. In the DSSCs, the Au nanoparticles generate field enhancement by surface-plasmon resonance rather than prolonged optical paths by light scattering. Fig. 3.14(a) shows the current density-voltage (J-V) characteristics and (b) the incident photon-to-current conversion efficiency (IPCE) spectra. The power-conversion efficiency of the DSSCs exhibits a maximum at the Au/TiO₂ mass ratio of 0.05 and rapidly decreases at 0.07 (Changwoo *et al.*, 2011).

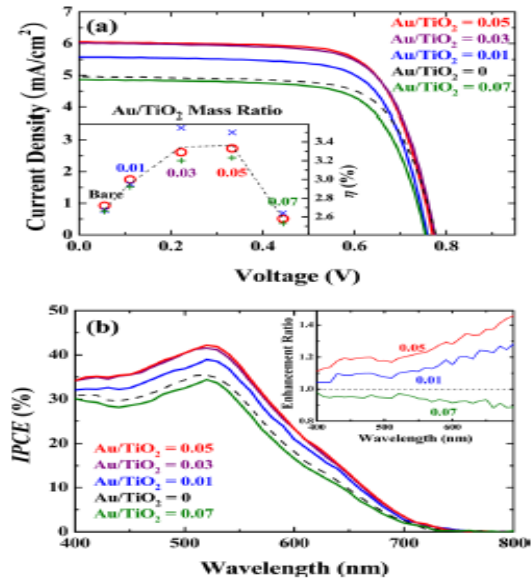


Fig. 3.14(a) shows the current density-voltage (J-V) characteristics and (b) the incident photon-to-current conversion efficiency (IPCE) spectra (Changwoo *et al.*, 2011).

Thambidurai *et al.* (2014a), reported that the improved morphology and electrical properties of the Sn-doped-TiO₂ film result in reduced shunt loss and interfacial charge recombination and hence enhanced photovoltaic performance. The inverted organic solar cell (IOSC) fabricated with Sn-doped-TiO₂ film showed a significant greater power conversion efficiency of 7.59 % compared to that of the TiO₂ film (6.70 %).

Amu (2014), observed from his thesis results that solar cells with tin iodide perovskite as the absorber can perform excellently well like at low ($\sim 10^{15} \text{ cm}^{-3}$) doping concentrations than its lead counterpart. An efficiency of >18% should be achievable with tin-based perovskite by preparing the device in an air tight condition in order to reduce oxidation of Sn. Solar cells with tin-based perovskites are not toxic unlike the lead based ones and at the same time, with careful engineering should be able to obtain similarly high efficiencies. In his effort to determine the effect of interface defect recombination, Amu (2014), went further, and carried out a check by removing the interface layer which accounts for both interface defect recombination. The J-V curve obtained by this check is as shown in Fig.3.15 with a higher efficiency of 8.17% compared to the previous set-up.

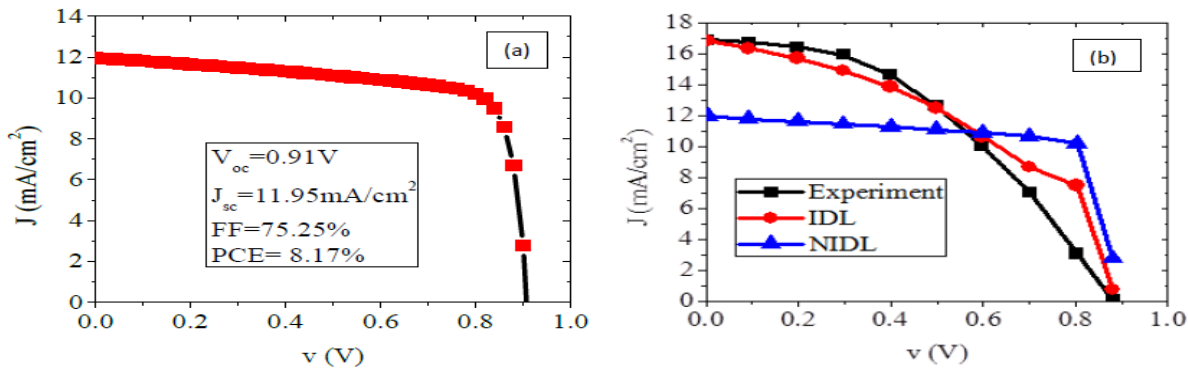


Fig. 3.15: (a) J-V curve of the photovoltaic structure without an interface layer (b) J-V curve plot of both the experiment and simulated p-i-n and p-n junction (Amu, 2014).

The Cs_2SnI_6 perovskite is an inexpensive and environmentally friendly material with high stability in air at temperatures up to 80 °C. Cs_2SnI_6 -based solar cells are also stable at room temperature for several months without any signs of performance decline. Nevertheless, their efficiency drops fast when exposed to 40 °C. Dye-sensitized solar cells were fabricated using the Z907 metal-organic complex as photosensitizer and Cs_2SnI_6 as hole transporter on mesoporous TiO_2 substrate. The power conversion efficiency remains constant at 3.3% when the solar cell is stored at room temperature in the dark. Successive current voltage measurements after exposure of the device to 40 °C for up to 200 hours revealed a marked effect on the photovoltaic performance (Andreas *et al.*, 2016). In order to render them suitable for commercial exploitation, the researchers recommended further studies which are needed to fully elucidate the mechanism of degradation, fine tune the corresponding interfaces and redesign the device for optimum long term efficiency.

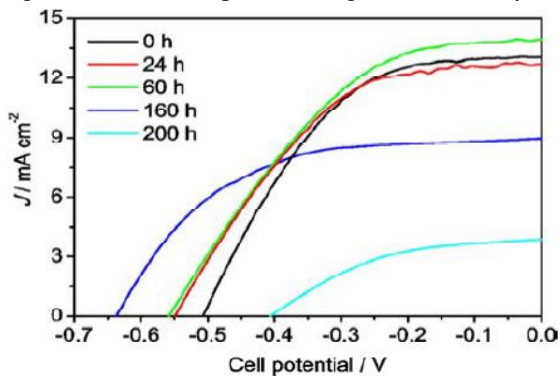


Fig. 3.16: Current-voltage curves for Cs_2SnI_6 -based solar cells after various exposure times at 40 °C.

As shown in Fig. 3.16. J-V measurements were carried out for sealed solar cells with lamellar structure FTO/compact

layer TiO_2 /mesoporous TiO_2 /Dye/Perovskite/Pt. Cells exhibited consistently high current densities of 13 mA cm^{-2} and efficiencies higher than 3% when stored in the dark (Andreas *et al.*, 2016).

Kasim *et al.* (2016), fabricated and enhanced Dye-sensitized solar cells (DSSCs) comprising mesoporous TiO_2 films and betalain pigments extracted from red *Bougainvillea glabra* flower as natural dye sensitizers by the intercalation of the plasmonic silver nanoparticles (Ag NPs) into the pores of mesoporous TiO_2 electrodes by successive ionic layer adsorption and reaction (SILAR) method. I-V characteristics of the devices were measured by solar simulator (AM1.5 at 100 mW/cm^2). The incorporation of the Ag nanoparticles into the pores of mesoporous TiO_2 electrodes with one SILAR deposition cycle of the Ag NPs produced the best plasmonic enhanced-DSSC giving a short-circuit current density (J_{sc}), fill factor (FF), and power conversion efficiency (PCE) of 1.01 mA cm^{-2} , 0.77, and 0.27 %, respectively. This development amounts to 50 % efficiency enhancement over the reference DSSC that had a short-circuit current density (J_{sc}), fill factor (FF), and power conversion efficiency (PCE) of 0.7 mA cm^{-2} , 0.57, and 0.18 %, respectively.

Fig. 3.17 shows the J-V and P-V characteristic curves of both the bare and intercalated plasmonic Ag NPs DSSCs. The photovoltaic performances of the cells are determined through the photovoltaic parameters (short-circuit current density (J_{sc}), open-circuit voltage (V_{oc}), fill factor (FF), and conversion efficiency (η), which are obtained from the J-V and P-V characteristic curves of the cells. The fill factor (FF) defined as the ratio of P_{max} and the product $J_{sc} \cdot V_{oc}$ shows curve squareness, and the closer to unity the fill factor is, the better cell quality will be.

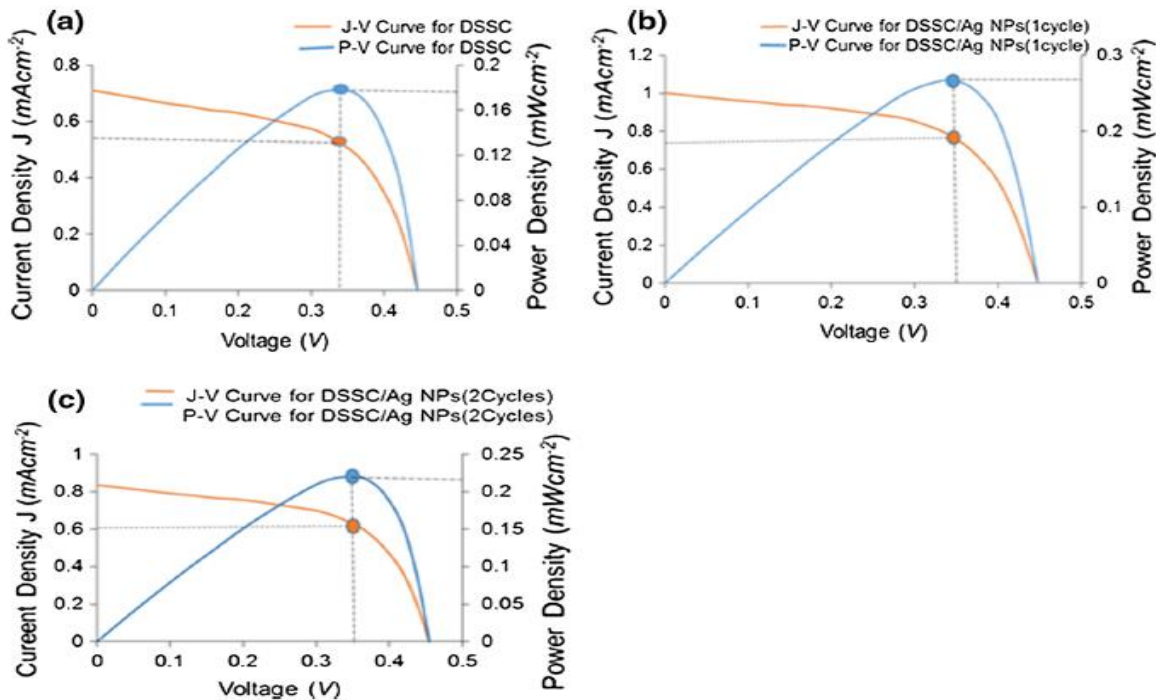


Fig. 3.17: J–V and P–V characteristic curves of (a) DSSC with bare TiO₂ electrode, (b) DSSC with one SILAR cycle TiO₂ intercalated Ag NPs electrode, and (c) DSSC with two SILAR cycles TiO₂ intercalated Ag NPs electrode (Kasim *et al.*, 2016).

Faruk *et al.* (2018), identified recent advancements on the impact of A-organic cations, B-inorganic cation, and X-anion substitutions on stability, efficiency, and photovoltaic performance of lead-free organic-inorganic halide perovskite. They stated that the major challenge associated with the conventional perovskite solar cells is the toxic nature of lead (Pb) used in the active layer of perovskite material and if lead continues to be used in fabricating solar cells, negative health impacts will result in the environment due to the toxicity of lead. Alternatively, lead free perovskite solar cells could give a safe way by substituting low-cost, abundant and non-toxic material. They conclude that structural modification has great impact on the band gap and the overall photovoltaic performance of the perovskite solar cells.

E. Zinc Oxide Based Solar Cells

ZnO is an attractive material for applications in electronics, photonics, acoustics, and sensing. In optical emitters, its high exciton binding energy (60 meV) gives ZnO an edge over other semiconductors such as GaN if reproducible and reliable p-type doping in ZnO were to be achieved, which currently remains to be the main obstacle for realization of bipolar devices. On the electronic side, ZnO holds some potential in transparent thin film transistors (TFTs) owing to its high optical transmittivity and high conductivity (Umit, 2010).

Lai *et al.* (2011), presents a new structure for nanorod DSSCs. ZnO nanorods and a ZnO film were grown using a one-step chemical-vapor deposition method. The ZnO film functioned as the TCO of the DSSC. The ZnO nanorod/ZnO film structure was sensitized with D149 or N719 dye and assembled into a DSSC. Two notable features in this new DSSC structure are: (1) the junction between the TCO film and the nanorods is completely

eliminated; (2) the TCO and the photoelectrode are made of the same material. Testing showed that under AM1.5 illumination, a short current density of 15.7 mA/cm² and a power conversion efficiency η of 1.82% can be achieved. The η is more than two times higher than the η reported earlier for ZnO-nanorod DSSCs with the same structure. Fig. 3.18 shows typical *I*-*V* curves of the new-structure and conventional-structure ZnO-nanorod DSSCs under AM1.5 (100 mW/cm²) illumination

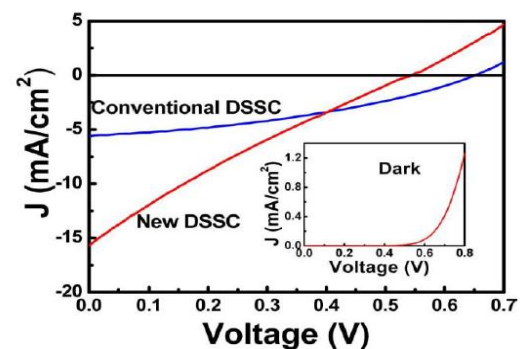


Figure 3.18: *I*-*V* curves of the ZnO-nanorod DSSC (Lai *et al.*, 2011).

Zinc Oxide thin films are formed by electrodeposition of Zinc Nitrate. Their structural and optical characteristics were confirmed using UV-VIS absorption and emission. The FTIR of ZnO was also investigated. Their photoconductive performance was verified which makes them promising candidates for Solar Cells (Sathya *et al.*, 2012).

Yuancheng (2015), has reviewed the research progress in ZnO Nanowires and their application for solar cells. He found that, a number of methods have been employed to

achieve ZnO nanostructured arrays and several attempts have been made to use ZnO in solar cells. In his opinion, more work is still needed to make further progress on the topic. First, the quality and stability of the ZnO nanowires need to be further improved. This will require even better control of the background conductivity, development of new growth methods and search for new acceptor dopants. Second, the techniques used in fabricating these solar cells have still to be optimized. Once these milestones are achieved, the ZnO nanowire arrays have great potential in improving the performance of solar cells.

Vanja *et al.* (2018), electrodeposited ZnO thin films to study the effects of different potentials applied during deposition. ZnO photoanodes were synthesized through electrodeposition at the potentials of -1.0 V (film A), -1.2 V (film B) and -1.4 V (film C). SEM images, XRD and UV-Vis analysis were conducted to reveal the morphologic, structural and optical properties of the films at three potentials. DSSCs were assembled and the photovoltaic parameters were obtained through J-V plots. DSSC with 0.031% of efficiency was demonstrated at -1.4 V of deposition potential.

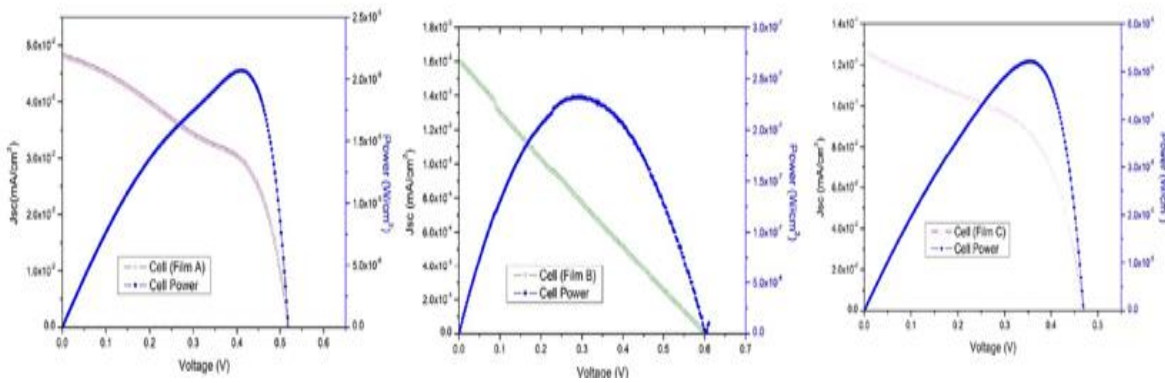


Fig. 3.19: J-V

measurements for the three dye cells Sample A, B and C

Fig. 3.19 reports the photocurrent density voltage (J-V) plots under the 100 mW/cm² illumination which shows the Pmax of 1.22 x 10⁻⁵, 2.32 x 10⁻⁷ and 3.07 x 10⁻⁵ (W/cm²) for sample A, B and C respectively (Vanja *et al.*, 2018).

of ZnO, the PCE was increased by 44.7% as shown in Fig. 3.20 (Mati *et al.*, 2019).

Mati *et al.* (2019), report on an efficient dye-sensitized mesoporous photoanode of Ti doped zinc oxide (Ti-ZnO) through a facile hydrothermal method. The crystallinity, morphology, surface area, optical and electrochemical properties of the Ti-ZnO were investigated using X-ray photoelectron spectroscopy, transmission electron microscopy and X-ray diffraction. It was observed that Ti-ZnO nanoparticles with a high surface area of 131.85 m² g⁻¹ and a controlled band gap, exhibited considerably increased light harvesting efficiency, dye loading capability, and achieved comparable solar cell performance at a typical nanocrystalline ZnO photoanode.

Babatunde *et al.* (2019), successfully deposited ZnS thin films on the glass substrate using a chemical bath deposition method. The effect of deposition time on optical and morphological characteristics of the films was investigated. The optical result shows the films have high transmittance, low reflectance in the visible region and also high optical band gap energy from 3.6 eV to 3.8 eV as the time of deposition increases.

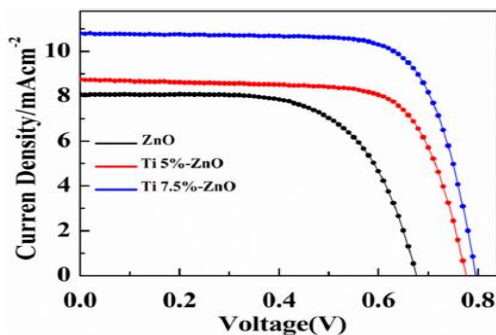


Fig. 3.20: I-V curves of ZnO, Ti(5%)-ZnO and Ti(7.5%)-ZnO nanoparticles based DSSCs, in both the active area is 0.25 and under (AM 1.5, 100 mW/cm²) illumination.

The increase in Jsc and Voc might be attributed to improved light harvesting efficiency of the photoanode, compared with the highest PCE value of the cell composed

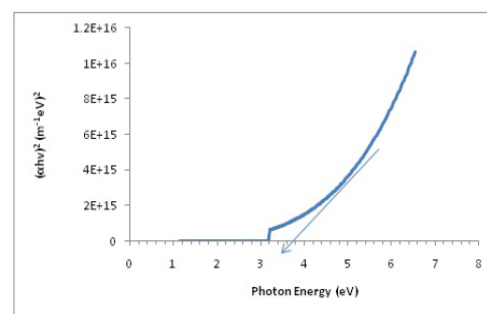


Fig. 3.21: Graph of hv (eV) against (αhv)² for ZnS thin film deposited for 1 hour

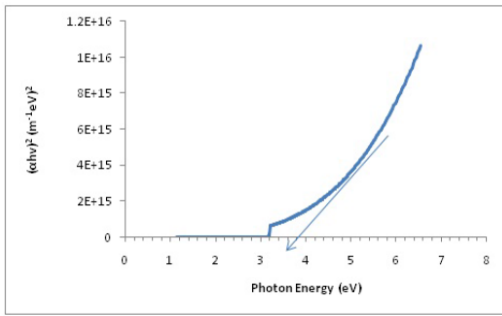


Fig. 3.22: The graph of $h\nu(\text{eV})$ against $(\alpha h\nu)^2$ for ZnS thin film deposited for 2 hours

As shown in Fig. 3.21 and 3.21, the spectral (Transmittance spectral and Reflectance spectral) read from 190nm to 1100nm. The transmittance spectrum increases in the visible region of wavelength from 400nm to 800nm and decreases in the infrared region above 800nm wavelength. The film deposited for 2 hours shows the highest transmittance while the one deposited for 3 hours show the lowest transmittance and a film deposited for 1 hour has a transmittance. Also, the reflectance spectra reveal that the film has the same percentage for all depositions time. The optical band gap energies of the film were extrapolated and show in Fig. 3.21 and 3.21 for the film deposited for 1 hour and 2 hours respectively. The values of band energies are 3.60eV and 3.70eV for the film deposited for 1 hour and 2 hours respectively (Babatunde *et al.*, 2019).

F. Nickel Oxide Based Solar Cells

The applications of Nickel oxide (NiO) today is found in semiconductors, capacitor-inductor devices, tuned circuits, transparent heat mirrors, thermistors and varistors, batteries, micro-supercapacitors, electrochromic and chemical or temperature sensing devices. It is used in preparation of nickel cermet, plastics and textiles, in nanowires, nanofibers and specific alloy and catalyst applications. It is also used as an antiferromagnetic layers, accelerators and radar absorbing materials, aerospace and active optical filters (Sani *et al.*, 2019; AzoNano, 2013). Pedram (2017), explore two different systems solar cells. The first system is a NiO mesoporous semiconductor photocathode sensitized with a biomimetic FeFe-catalyst and a coumarin C343 dye, which was tested in a solar fuel device to produce hydrogen. This system is the first solar fuel device based on a biomimetic FeFe-catalyst and it shows a Faradic efficiency of 50% in hydrogen production. Cobalt catalysts have higher Faradic efficiency but their performance due to hydrolysis in low pH condition is limited. The second system is a photoanode based on the nanostructured hematite/magnetite film, which was tested in a photoelectrochemical cell. This hybrid electrode improved the photoactivity of the photoelectrochemical cell for water splitting. He added that, the metal oxide semiconductors are promising active materials in solar cells and solar fuel devices due to their abundance, stability, non-toxicity, and low-cost.

Kingsley *et al.* (2018), fabricated Metal oxide TiO_2/NiO heterojunction solar cells using the spray pyrolysis technique. The optoelectronic properties of the heterojunction were determined. The fabricated solar cells

exhibit a short-circuit current of 16.8 mA, open-circuit voltage of 350 mV, fill factor of 0.39, and conversion efficiency of 2.30% under $100\text{mW}/\text{cm}^2$ illumination. Therefore, their study will help advance the course for the development of low-cost, environmentally friendly, and sustainable solar cell materials from metal oxides. As shown in Figure 3.23, the J-V characteristic at room temperature in the dark shows that the forward current of the cells increases slowly with increasing voltage. Fig. 3.24 depicts generation of electricity by a solar cell using a P-N junction.

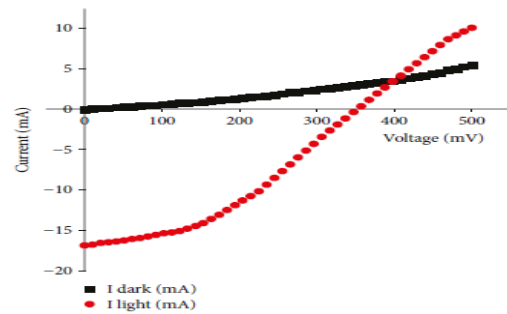


Fig. 3.23: Typical I-V curve for the prepared TiO_2/NiO heterojunction thin-film solar cell under illumination and in the dark (Kingsley *et al.*, 2018)

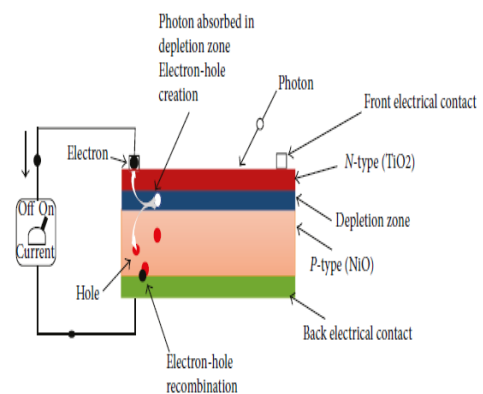


Fig. 3.24: Solar cell generation of electricity using a P-N junction (Kingsley *et al.*, 2018).

Ukoba *et al.* (2018a), focused on the experimental optimization of nanostructured nickel oxide (NiO) for solar cell applications. The optimization procedure involved the variation of the precursor concentrations of nickel acetate with attendant measurement of the properties of nickel oxide films. The films were spray deposited on glass substrate. Nickel acetate precursor was used at a substrate temperature of 350°C . Optical studies showed that transmittance decreased with increasing concentration from 80 % to 71 %. Optical band gap energy was between 3.94 eV to 3.38 eV as precursor concentration increased, revealing the effect of varied concentrations on NiO film properties. Optimized results obtained are precursors in the development of low cost, efficient, durable solar cell fabrication for developing countries.

Ukoba *et al.* (2018b) report modelling and theoretical validation of a fabricated NiO/TiO_2 P-N heterojunction solar cell. The solar cell equations were modelled and thereafter theoretical validation of the fabricated solar cells was performed. Modelling tools were used to validate the influence of NiO material features such as deposition temperature, voltage and defect densities on the performances of an $\text{ITO}/\text{TiO}_2/\text{NiO}$ heterojunction solar

cell structure. The working points used included a temperature of 350 °C, illumination of 1000 W/m² using an AM1.5 lamp, with voltage range of 0 to 1.5 volts. The output gave Voc of 0.1445 V, Jsc of 247.959195E-6 mA/cm² and FF of 37.87 % and Voc 0.7056 and Jsc 28.366911 mA/cm² when both contacts were added. This opens a new frontier for modelling of metal oxide based thin film solar cells especially NiO thin film solar cells. The findings therefore enhance the quest to develop affordable and sustainable energy and encourage further research in solar cell technologies in low-income countries.

Ukoba *et al.* (2018c), investigate the optoelectronic properties of nanostructured TiO₂/NiO heterojunction solar cells. The heterojunction was fabricated using spray pyrolysis technique at above 350 °C on Indium Tin Oxide substrate. The X-ray diffraction shows that the heterojunctions have a polycrystalline cubic structure with a preferred orientation along the (1 1 1) and (2 0 0) planes. The elemental properties show the presence of TiO₂ and NiO. The optical band gap, refractive index and other optoelectronic properties were also investigated. These findings will enhance the study of cheap, efficient and sustainable alternate materials for solar energy development and affordable energy in developing countries.

G. Polymer Based Solar cells

The solar cell can be prepared entirely in the ambient atmosphere by solution processing without the use of vacuum coating steps and can be operated in the ambient atmosphere with good operational stability under illumination (1000 W m⁻², AM1.5G, 30 °C, 35 ± 5 % relative humidity) for 100 hours with a 20% loss in efficiency with respect to the initial performance. The dark storability (darkness, 25 °C, 35 ± 5 % relative humidity) has been shown to exceed six months without notable loss in efficiency. The devices do not require any form of encapsulation to gain stability while a barrier for mechanical protection may be useful. The devices are based on soluble zinc oxide nanoparticles mixed with the thermo-cleavable conjugated polymer poly-[3-(2-methylhexan-2-yl)-oxy-carbonyldithiophene] (P3MHOCT) that through a thermal treatment is converted to the insoluble form poly(3-carboxydithiophene) (P3CT) that generally gives stable polymer solar cells. The devices employed a solution based silver back electrode. the devices gave a reasonable current and a high voltage to begin with (Fig. 3.25) (Krebs *et al.*, 2008).

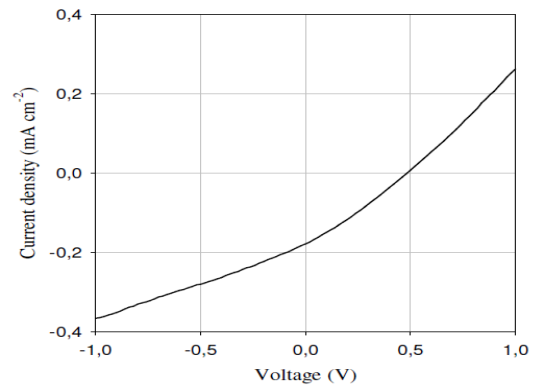


Fig. 3.25: IV characteristics of an as-prepared device on a glass substrate with an active area of 1 cm². Test conditions were 1000 W m⁻², AM1.5G, 72 ± 2 °C, 35 ± 5 % relative humidity, ambient atmosphere (Krebs *et al.*, 2008).

Thambidurai *et al.* (2013), demonstrate solution-processed Ga-doped-ZnO incorporated as an interfacial electron transport layer into inverted organic solar cells with active layers comprising either PCDTBT or PTB7 mixed with PC71BM. The 5.03 % Ga-doped-ZnO showed the best efficiencies at 5.56 and 7.34 % for PCDTBT and PTBT polymers respectively. In another similar study, Thambidurai *et al.* (2014), reported that, the 0.05 wt% polyethylene oxide-modified Zn-doped-TiO₂ device shows a significantly increased power performance conversion efficiency of 8.10 % compared to that of the Zn-doped-TiO₂ (7.67 %) device.

The BHJ-OSC devices constructed in their study (Hendrik *et al.*, 2015) comprised of successive (bottom up) layers of (3,4-ethylenedioxythiophene):poly (styrenesulfonate) or PEDOT:PSS, a blend of poly (3-hexylthiophene) or P3HT and [6,6]-phenyl butyric acid methyl ester or PCBM, zinc oxide or ZnO nanoparticles and aluminum (Al) metal top electrode. These layers were deposited on ITO (indium tin oxide) coated glass substrates. The device construction was also inverted (top down) in order to evaluate the effect of inversion on the power conversion efficiency and the general performance of the devices. The devices were annealed at 155 °C either before (pre-annealed) or after (post-annealed) the deposition of the Aluminium top electrode. Post-annealed devices showed improved PV (photovoltaic) characteristics when compared to pre-annealed devices.

Chemical bath-deposited cadmium sulfide (CdS) thin films were employed as an alternative hole-blocking layer for inverted poly(3-hexylthiophene) (P3HT) and phenyl-C61-butyric acid methyl ester (PCBM) bulk heterojunction solar cells. CdS films were deposited by chemical bath deposition and their thicknesses were successfully controlled by tailoring the deposition time. The influence of the CdS layer thickness on the performance of P3HT:PCBM solar cells was systematically studied. The short circuit current densities and power conversion efficiencies of P3HT:PCBM solar cells strongly increased until the thickness of the CdS layer was increased to ~70 nm. This was attributed to the suppression of the interfacial charge recombination by the CdS layer, which is consistent with the lower dark current found with the

increased CdS layer thickness (Murugathas *et al.*, 2019). The J-V characteristics of the solar cells fabricated with different CdS film thicknesses under simulated illumination of 100 mW/cm² (one sun) are shown in Fig. 3.26.

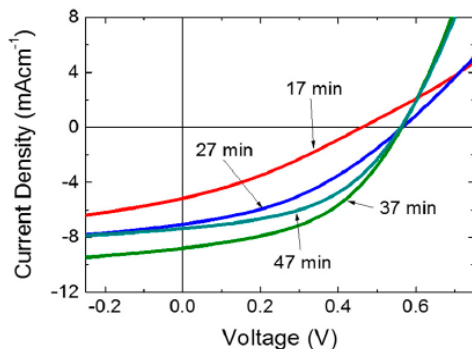


Figure 3.26: J-V curve ITO/CdS/P3HT:PCBM blend/PEDOT:PSS/MoO₃/Ag devices with different CdS deposition times.

H. Silver Nanoparticles Based Solar Cells

Jack *et al.* (2011), demonstrated a novel approach, to fabricate silver nanoparticles for light trapping applications in silicon based solar cells. The nanoparticles have been synthesized using chemical reduction reaction. They reported that deposition of the silver nanoparticles on to a conventional bulk silicon solar cells shows an increase in the quantum efficiency at longer wavelength, indicating the utilisation of incident radiation that is normally lost in poor absorbing silicon.

An approach to transfer Ag NPSMs from aqueous solution to organic solvents, especially to CB was developed: 10 mL as-prepared aqueous Ag NPSM solution is centrifuged at 6000 rpm for 15 minutes. The precipitate is then dispersed in 3 mL water and mixed with 3 mL hexane and 0.2 mL oleylamine by vigorous stirring for 30 minutes. After standing for 2 h, the resulting upper layer is washed by ethanol twice through centrifugation at 8500 rpm for 15 minutes. The precipitate is finally dispersed in 1 mL CB by ultrasonic bath for 30 minutes. Upon adding glycerol to the hybrid PEDOT:PSS-Ag NPSM films, the *J*_{sc} increases from 1.65 mA/cm² to around 2 mA/cm² and the *V*_{oc} decreases from 0.55 V to 0.45 V (Zhixiong, 2014).

The enhancement in efficiency of dye sensitized solar cells decorated with size-controlled silver nanoparticles based on anthocyanins as light harvesting pigment through successive ionic layer adsorption and reaction (SILAR) was demonstrated. Studies indicate that, the short-circuit current density (*J*_{sc}) and open-circuit voltage (*V*_{oc}), of DSSCs containing AgNPs were significantly improved. The photovoltaic (PV) performance decreased with increasing size of AgNPs from one SILAR cycle to two SILAR cycles, the best performance was achieved using the anode prepared with one SILAR cycle. An enhancement of 35.8 % was achieved when the thickness was around 16 nm (one SILAR) over the bare FTO device. When the size of AgNPs was around 32 nm (two SILAR), an enhancement of 10.4% was recorded over the reference device. It is shown from Fig. 3.27, that the mixed films

containing Ag particles exhibit an increase in the power conversion efficiency from 10.4 to 35.8% (Danladi *et al.*, 2016).

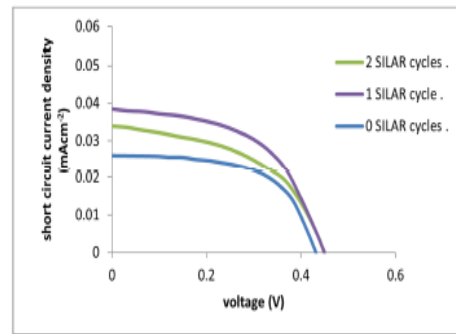


Fig. 3.27: The photocurrent density–voltage (J–V) curves with varying SILAR cycles (Danladi *et al.*, 2016)

IV. CONCLUSION

In recent years, photovoltaic cell technology has grown extraordinarily as a sustainable source of energy, as a consequence of the increasing concern over the impact of fossil fuel-based energy on global warming and climate change. The year 2017 was a landmark one for solar photovoltaics (PV) where the world added more capacity from solar PV than from any other type of power generating technology. More solar PV was installed than the net capacity additions of fossil fuels and nuclear power combined. Solar cells are found applicable in lighting, communications, electricity for remote areas, disaster relief, scientific experiments, water Pumping, charging vehicle batteries, signal systems, refrigerators, small DC appliances, ATMs and telephone booths etc. So many materials are reported to be useful in solar cells fabrications by contemporary researchers. Materials like silicon oxides, cadmium sulphide, copper sulphide, cuprous sulphide, nickel oxide, zinc oxide, silver nanoparticles, titanium dioxides, lead, gallium arsenide, perovskite, graphene, aluminium oxide, copper oxide, zinc sulphide, cadmium telluride, copper indium diselenide and many more are all reported to be good materials for solar cells manufacture. The search for other materials and ways of improving the efficiencies of the existing ones is underway.

REFERENCES

- [1] Abdin, Z. Alim, M. A. Saidur, R. Islam, M. R., Rashmi, W., Mekhilef, S. and Wadi, A. (2013). Solar energy harvesting with the application of nanotechnology. *Renewable and Sustainable Energy Reviews*, 26(2013)837–852.
- [2] Adriano, M., Izete, Z. (2012). Development of Silicon Solar Cells and Photovoltaic Modules in Brazil: Analysis of a Pilot Production. *Materials Research*, 15(4): 581-588.
- [3] Amu, T. L. (2014). Performance Optimization of Tin Halide Perovskite Solar Cells Via Numerical Simulation. Department of Theoretical Physics African University of Science and Technology, Abuja. "Unpublished".
- [4] Andreas, K., Dorothea, P., Maria, A., Athanassios, G. K., Polycarpos, F. (2016). Stress tests on dye-

- sensitized solar cells with the Cs_2SnI_6 defect perovskite as hole-transporting material. *Energy Procedia*, 102:49 – 55.
- [5] Anil, R. K., Suresh, M. S. and Nagaraju, J. (2001). Measurement of AC Parameters of Gallium Arsenide (GaAs/Ge) Solar Cell by Impedance Spectroscopy. *IEEE Transactions on Electron Devices*, 48(9):2177-2179.
- [6] Ashour, A. (2006). The Physical Characteristics of $\text{Cu}_2\text{S}/\text{Cds}$ Thin-Film Solar Cell. *Journal of Optoelectronics and Advanced Materials*, 8(4):1447 – 1451.
- [7] AzoNano, (2013), Nickel Oxide (NiO) Nanoparticles: Properties, Applications retrieved from www.azonano.com/article.aspx?ArticleID=3378 on 7th February, 2019.
- [8] Babatunde, R. A., Bolanle, Y. I. and Adegboyo, O. O. (2019). Effects of Deposition Time of ZnS Thin Film on Optical and Morphological Properties of ZnS Deposited by Chemical Bath Deposition Method for Photovoltaic Application. *Journal of Theoretical & Applied Physics*, 1(2019):38-45.
- [9] Bülent, M. B. and Brian, M. (2014). Brief review of cadmium telluride based photovoltaic technologies. *Journal of Photonics for Energy*, 4:1-11.
- [10] Changwoo, N., Hongsik, C., Jongmin, K., Dae-Ryong, J., Chohui, K., Joonhee, M., Byungjoo, L. and Byungwoo, P. (2011). The effects of 100 nm-diameter Au nanoparticles on dye-sensitized solar Cells. *Applied Physics Letters*, 99(25):1-11.
- [11] Choubey, P.C., Oudhia, A. and Dewangan, R. (2012) A Review: Solar Cell Current Scenario and Future Trends. *Recent Research in Science and Technology*, 4, 99-101.
- [12] Danladi, E., Joshua, A. O., Gabriel, O. O. and Ezeoke, J. (2016). Plasmon-Enhanced Efficiency in Dye Sensitized Solar Cells Decorated with Size-Controlled Silver Nanoparticles Based on Anthocyanins as Light Harvesting Pigment. *Journal of Photonic Materials and Technology*, 2(1): 6-13.
- [13] Davood, S., Bahman, H. and Devendra, K. S. (2011). Low-Temperature a-Si:H/GaAs Heterojunction Solar Cells. *IEEE Journal of Photovoltaics*, 1(1):104-107.
- [14] Enama, F. M. T., Rahmana, K. S., Kamaruzzamana, M. I., Sobayela, K., Chelvanathana, P., Baisa, B., Akhtaruzzamanb, M., Alamoudc, A.R.M., Amin, N. (2017). Design prospects of cadmium telluride/silicon (CdTe/Si) tandem solar cells from numerical simulation. *Optik*, 139(2017): 397–406.
- [15] Ezenwa, I. A. and Okereke, N. A. (2011). Optical Properties of Cadmium Sulphide (Cds), Copper Sulphide (Cus) and (Cds/Cus) Thin Films and their Applications in Photovoltaic Technology. *Nigerian Journal of Solar Energy*. 22:61-65.
- [16] Faruk, S., Suhaidi, S., Hong, N. L. and Abubakar, O. M. (2018). Advancement on Lead-Free Organic-Inorganic Halide Perovskite Solar Cells: A Review. 11(1008):1-17.
- [17] Hendrik, C.S., Odireleng, M. N., Pontsho, S. M., Mokhotjwa, S. D. and Bakang, B. M. (2015). P3HT:PCBM Based Solar Cells: A Short Review Focusing on ZnO Nanoparticles Buffer Layer, Post-Fabrication Annealing and an Inverted Geometry. *Journal of Materials Science and Engineering B*, 5(1-2):12-35.
- [18] Holly, F. Z., William, R. E., Abdelaziz, B., Olivia, K. H., Joseph, A. W., Alexander, A. P., David, B. G. and Rizia, B. (2016). Improving Light Harvesting in Dye-Sensitized Solar Cells Using Hybrid Bimetallic Nanostructures. *ACS Photonics*, 3:385–394.
- [19] Jack, B. Mayandi, J. and Annett, T. (2011). Chemical Synthesis of Silver Nanoparticles for Solar Cell Applications. *Physica Status Solidi*, 8(3):924-927.
- [20] José A. L., Ana M. D. and Rafael P. C (2019). Materials for Photovoltaics: State of Art and Recent Developments. *International journal of molecular sciences*, 20(97):1-42.
- [21] Karla, G. Z., Patricia, G. Z., Osvaldo, M., Francisco, M., José, A. A., Luis, A. M., Hugo, M. G., Salvador, G., Jorge, S. and Gerardo, C. (2018) CdS/CdTe Heterostructures for Applications in Ultra-Thin Solar Cells. *Materials*, 11(1788):1-8.
- [22] Kasim, U. I., Bukola, J. J., Umaru, A., Mohammed, I. K. and Noble, A. (2016). Plasmonic effect of silver nanoparticles intercalated into mesoporous betalain-sensitized-TiO₂ film electrodes on photovoltaic performance of dye-sensitized solar cells. *Mater Renew Sustain Energy*, 5(10):1-9.
- [23] Kingsley, O. U., Freddie, L. I. and Andrew, C. E. (2018). Fabrication of Affordable and Sustainable Solar Cells Using NiO/TiO₂ P-N Heterojunction. *International Journal of Photoenergy* Vol. 2018, pp. 1-7.
- [24] Krebs, F. C., Thomann, Y., Thomann, R., and Andreassen, J. W. (2008). A simple nanostructured polymer/ZnO hybrid solar cell - preparation and operation in air. *Nanotechnology*, 19(42):424013-424024.
- [25] Lewis, F. and Larry, P (2010). *Solar Cells and Their Applications*. 2nd Edition, A John Wiley & Sons, Inc., Publication, Canada.
- [26] Mahfoud, A., Mohamed, F., Saad, M., Farid, D. (2015). Effect of Temperature on the GaInP/GaAs Tandem Solar Cell Performances. *International Journal of Renewable Energy Research*, 5(2): 629-635.
- [27] Mati, U., Mingdeng, W., Fengyan, X. and Matiullah, K., (2019). Efficient Dye-Sensitized Solar Cells Composed of Nanostructural ZnO Doped with Ti. *Catalysts*, 9(273):1-11.
- [28] Mayank, J. and Reeta, V. (2017). Black Silicon Photovoltaics: Fabrication Methods and Properties. *International Journal of Research in Engineering and Science (IJRES)*. 5(5):62-72.
- [29] Meier, J., Spitznagel, J., Krolla, U., Buchera, C., Fay, S., Moriarty, T. and Shah, A. (2004). Potential of amorphous and microcrystalline silicon solar cells. *Thin Solid Films*, 451-452.
- [30] Mostafa, F., Shereen, M. A., Tarek, A. (2018). Efficiency Enhancement of GaAs Solar Cell using Si₃N₄ Antireflection Coating. *Journal of Advanced Research in Materials Science*, 42(1):1-7.

- [31] Mrityunjoy. K. R., Sajal, S., Santigopal, M. (2015). Improvement of Quantum Efficiency and Reflectance of GaAs Solar Cell. *International Journal of Engineering Research and General Science*, 3(2):641-646.
- [32] Murugathas, T., Selvadurai, L., Kailasapathy, B., Dhayalan, V. and Punniamorthy, R. (2019). Polymer/Fullerene Blend Solar Cells with Cadmium Sulfide Thin Film as an Alternative Hole-Blocking Layer. *Polymers*, 11(460):1-9.
- [33] Nura, L. C. and Kamarulazizi, I. (2015). Concept of Bee-Eyes Array of Fresnel Lenses as a Solar Photovoltaic Concentrator System. *Journal of Photonics*, 1-8.
- [34] Pedram, G. (2017). Advanced Metal Oxide Semiconductors for Solar Energy Harvesting and Solar Fuel Production. Luleå University of Technology, Graphic Production, Sweden. "Unpublished".
- [35] Plakhotnyuk, M., Davidsen, R. S., Schmidt, M. S., Malureanu, R., Stamate, E. and Hansen, O. (2016). Lifetime of Nano-Structured Black Silicon for Photovoltaic Applications. In *Proceedings of 32nd European Photovoltaic Solar Energy Conference and Exhibition*, 764-767.
- [36] REN21, (2018). *Renewables 2018 Global Status Report*, Paris REN21 Secretariat, Paris France.
- [37] Sani, G. D., Yakubu, A. and Sahabi, S. (2019). Nickel Oxide (NiO) Devices and Applications: A Review. *International Journal of Engineering Research & Technology (IJERT)*, 8(04):461-467.
- [38] Satheesh, K. (2018). Applications of photovoltaic systems. OPEN University UK. "Unpublished"
- [39] Sathya, M., Claude, A., Govindasamy, P. and Sudha, K. (2012). Growth of pure and doped ZnO thin films for solar cell applications. *Advances in Applied Science Research*, 3(5):2591-2598.
- [40] Sekhar, C. R. and Kaushik, M. (2013). Cadmium Telluride (CdTe) Thin Film for Photovoltaic Applications. *International Journal of Chemical Engineering and Applications*, 4(4):183-186.
- [41] Shruti, S., Kamlesh, K. J. and Ashutosh, S. (2015). Solar Cells: In Research and Applications—A Review. *Materials Sciences and Applications*, 6:1145-1155.
- [42] Silicon Valley Toxics Coalition, (2019). *Toward a Just and Sustainable Solar Energy Industry*. San Francisco.
- [43] Soteris, K. (2009). *Solar Energy Engineering Processes and System*, 1st Ed., Elsevier Inco. UK. Pp30.
- [44] Thambidurai, M., Jun, Y. K., Jiyun, S., Youngjun, K., Hyung-jun, S., Chan-mo, K., Muthukumarasamy, N., Dhayalan, V. and Lee, C. (2013). High Performance Inverted Organic Solar Cells with Solution Processed Ga-Doped-Zno as an Interfacial Electron Transport Layer. *Journal of Materials Chemistry C*, 1(8161):36.
- [45] Thambidurai, M., Jun, Y. K., Jiyun, S., Youngjun, K., Hyung-jun, S., Chan-mo, K., Muthukumarasamy, N., Dhayalan, V., Victor, W. B., Stefan, A. L. W. and Lee, C. (2014a). Enhanced Power Conversion Efficiency Of Inverted Organic Solar Cells by Using Solution Processed Sn-Doped-Tio₂ as an Electron Transport Layer. *Journal of Materials Chemistry A*, 2(11426):37.
- [46] Thambidurai, M., Jun, Y. K., Jiyun, S., Youngjun, K., Hyung-jun, S., Chan-mo, K., Muthukumarasamy, N., Dhayalan, V., Victor, W. B., Stefan, A. L. W. and Lee, C. (2014b). High Performance Inverted Organic Solar Cells With Polyethylene Oxide-Modified Zn-Doped-Tio₂ as an Electron Transport Layer. *Nanoscale*, 6(8585):38.
- [47] Ukoba, O. K, Inambao, F. L. and Eloka-Eboka, A. C. (2018a). Experimental Optimization of Nanostructured Nickel Oxide Deposited by Spray Pyrolysis for Solar Cells Application. *International Journal of Applied Engineering Research*, 13(6):3165-3173.
- [48] Ukoba, O. K. and Inambao, F. L. (2018b). Modeling of Fabricated NiO/TiO₂ P-N Heterojunction Solar Cells. *International Journal of Applied Engineering Research*, 13(11): 9701-9705.
- [49] Ukoba, O. K. and Inambao, F. L. (2018c). Study of Optoelectronic Properties of Nanostructured TiO₂/NiO Heterojunction Solar Cells. *Proceedings of the World Congress on Engineering and Computer Science*, (I):23-25.
- [50] Umit, O. (2010). ZnO Devices and Applications: A Review of Current Status and Future Prospects. *Proceedings of the IEEE*, 98(7):1255-1268.
- [51] Vanja, F. N., Antonio, P. S. S., Francisco, L. and Gessé, O. (2018). Effects of Potential Deposition on the Parameters of ZnO dye-sensitized Solar Cells. *Materials Research*, 21(4):1-8.
- [52] Vishnuvardhanan, V. and Dunbar, P. B. (2013). Optical and Electronic Simulation of Gallium Arsenide/Silicon Tandem Four Terminal Solar Cells. *Solar Energy* 97, 85-92.
- [53] Xiaoqiang, L. Shengjiao, Z. Peng, W. HuikaiZhong, Z. W.,Hongsheng, C. Erping, L. C. and Shisheng, L. (2018). High performancesolar cellsbased on grapheme/GaAs heterostructures. Department of Information Science and Electronic Engineering, Zhejiang University, Hangzhou 310027, China. "Unpublished".
- [54] Yuancheng, Q. (2015). ZnO Nanowires and Their Application for Solar Cells. Retrieved from www.researchgate.net/publication/221913392 on 05/05/2019.
- [55] Zhixiong, C. (2014). Silver nanoprisms in plasmonic organic solar cells. Micro and nanotechnologies/Microelectronics. Ecole Centrale Marseille, English. NNT. 2014ECDM0015.